Exploring the Mechanisms of Acupuncture-Induced Lowering of Blood Pressure Through Positron Emission Tomography and RNA Sequencing of the PVH

Jing Li
Guangzhou University of Chinese Medicine
Chong Peng
Guangzhou University of Chinese Medicine
Dongjian Lai
Guangzhou University of Chinese Medicine
Yajing Fang
Guangzhou University of Chinese Medicine
Daihong Luo
Shenzhen Hospital of Beijing University of Chinese Medicine
Zunming Zhou
Guangzhou University of Chinese Medicine
Chenyun Li
Guangzhou University of Chinese Medicine
Xinsheng Lai (✉ lai1023@163.com)
Guangzhou University of Chinese Medicine

Research Article

Keywords: manual acupuncture, hypertension, PET-CT, transcriptome, paraventricular nucleus of the hypothalamus

Posted Date: December 3rd, 2020

DOI: https://doi.org/10.21203/rs.3.rs-112631/v1

Abstract

Manual acupuncture (MA) can be used to manage high blood pressure, however, the underlying molecular mechanism remains unknown. To explore the mechanism of acupuncture in the treatment of hypertension, we used Wistar Kyoto rats (WKYs) and spontaneously hypertensive rats (SHRs) that were subject to either MA stimulation or the corresponding sham procedure as a negative control (sham-MA) for 1 week. Blood pressure was recorded regularly. After 7 days of treatment, PET-CT scans were used to detect brain areas where glucose metabolism was significantly regulated. Additionally, the differentially expressed genes(DEGs) of a specific brain region—the paraventricular hypothalamic nucleus (PVH)—were evaluated by transcriptomics, and verified with quantitative PCR (qPCR). Eight overlapping DEGs were found between the WKY, SHR, and MA groups. The DEGs were then annotated with the Gene Ontology (GO) and the Kyoto Encyclopedia of Genes and Genomes (KEGG) databases. qPCR was used to verify the DEGs. These genes may lower blood pressure by regulating angiotensin, endothelial function and inflammation, ect. This study reveals MA regulates multiple biological processes and genes of the PVH, and provides a solid theoretical basis for exploring the mechanisms by which MA manages hypertension.

Introduction

In most international guidelines, the measurement for diagnosing hypertension is that systolic blood pressure is no less than 140 mm Hg and/or diastolic blood pressure is no less than 90 mm Hg[1,2]. So far, the reasons for the development of hypertension have mainly been related to increased exposure to environmental factors that cause high blood pressure, including excessive consumption of salt, alcohol, and calories. Elevated blood pressure remains the largest single factor in the global burden of disease and mortality, killing 94 million people each year, according to the latest data[3]. The global prevalence of high blood pressure is expected to increase by about 10% in the next two decades, corresponding to an estimate of 560 million people that will suffer from hypertension[4]. If hypertension is not diagnosed and managed in time, it can lead to myocardial infarction, stroke, kidney failure, and even death[5-7].

Acupuncture is an effective alternative therapy for the treatment of hypertension[8-10]. Our previous animal trials showed that manual acupuncture (MA) at the KI3 position can effectively reduce systolic blood pressure (SBP) and diastolic blood pressure (DBP) in spontaneously hypertensive rats (SHRs)[11]. Moreover, our previous PET-CT study found that acupuncture may regulate blood pressure by changing the brain glucose metabolism of SHRs[12]. However, the underlying molecular mechanisms of acupuncture treatment for hypertension have not been widely described.

RNA sequencing is a new technical method that locates and quantifies the transcriptome through microarrays, which can digitally measure the existence and prevalence of transcripts[13,14]. Recent transcriptomic studies have found that acupuncture affects the mRNA levels of multiple differentially expressed genes (DEG) in the brain of the rat and regulates multiple biological processes, including inflammation, oxidative stress, and vascular endothelial function[15,16]. However, it has not been reported which signaling pathways and genes in specific brain regions are affected by MA at KI3.

Here, we studied the changes in cerebral glucose metabolism of 15-week-old SHRs after MA at KI3, by isolating the PVH, which is the target brain region of acupuncture, and performing transcriptomic sequencing. First, we determined the DEG. Then, we annotated the identified genes according to their Gene Ontology (GO) and Kyoto Encyclopedia of Genes and Genomes (KEGG) pathway classification, followed by verifying the expression levels of these DEGs by qPCR. This is a promising transcriptome study of the PVH after acupuncture at KI3, and may help us understand the role of acupuncture in the treatment of hypertension.

Results

Effects of Manual Acupuncture (MA) on Blood Pressure (BP)

To evaluate the antihypertensive effect of MA, the BP of the rats was measured at 30, 60, and 90 minutes after the first treatment. As shown in Figure1 a and b, the SBP and DBP of the MA group were significantly reduced at 30 and 60 minutes after acupuncture compared with the SHR group. Therefore, for the following 6 days, the BP of the rats was repeatedly measured 30 minutes after daily acupuncture. Compared with the SHR group, acupuncture at KI3 significantly reduced the SBP and DBP of rats from the first day to the seventh day, as shown in Figure1 c and d.

Changes to Glucose Metabolism in the Brain of SHRs

Glucose metabolism was significantly increased in the hypothalamus, thalamus, dorsal thalamus and olfactory bulb of the SHR group compared with the WKY group, but decreased in other regions including the cingulate cortex, cingulate gyrus, and motor cortex(Table 1 and Figure2 a). However, compared with the SHR group, the MA group showed significantly reduced glucose metabolism in the accumbens nucleus, hypothalamus, olfactory bulb, thalamus, anterior commissure, dorsal thalamus, and hypothalamus tuberal regions, and increased glucose metabolism in the cerebellum posterior lobe and visual cortex(Table 2 and Figure2 b). Furthermore, compared with the SHR group, the Sham-MA group showed significantly reduced glucose metabolism in the basal ganglia, caudate putamen, olfactory bulb, prefrontal cortex and orbital cortex, while this increased in the medulla oblongata(Table 3 and Figure2 c).

Filter of sequencing raw reads

Transcriptomic sequencing was conducted to analyze the expression profile of the hypothalamus in the WKY, SHR group, and MA groups. A total of 955.27 Mbp of raw reads were obtained. The percentage of clean reads Q20 and Q30 (the ratio of the quality values of the reads that were respectively larger than 20 and 30 compared to the total reads) indicated that the sequence was of high quality and could be used for subsequent analyses (supplementary table 2 and supplementary figure 1). After filtering the invalid readings, 267.75, 267.54, and 266.12 Mbp of clean readings were respectively obtained from the WKY, SHR group, and MA group. The proportion of clean reads were 82.9%–84.15% in the WKY group, 84.15%–86.29% in the SHR group, and 81.2%–84.69% in the MA group. The clean read ratio of the rat genome suggested that the sequencing depth was satisfactory for the analysis of the differentially expressed genes between the groups of rats.

Differentially expressed genes in the hypothalamus of WKY, SHR, and MA

In order to study the regulation of DEGs between the WKY, SHR, and MA groups, DEGs in the hypothalamus were analyzed. DEseq2 algorithms were based on negative binomial distribution to detect the DEGs by applying a fold change ≥2.00 and an adjusted p-value ($p \leq 0.05$). The statistics of the number of DEGs are shown by heatmap (Figure 3 a, d), scatter plot (Figure 3 b, e), and volcano plot (Figure 3 c, f). There were 695 DEGs in the SHRs relative to the WKY rats, with 375 upregulated genes and 320 downregulated genes. A total of 120 DEGs were found in the MA rats relative to the SHRs, with 72 upregulated genes and 48 downregulated genes. A Venn analysis was used to study the possible genes involved in reducing blood pressure as a result of acupuncture. We found that when applying MA treatment, we could abolish the upregulation of 5 of the 375 genes upregulated in SHRs compared to wild type rats. Correspondingly, MA treatment was able to counteract the downregulation of 3 of the 320 downregulated genes in SHRs (Figure 3 g, h).

Gene Ontology and Kyoto Encyclopedia of Genes and Genomes analysis

To investigate the function of the DEGs, Gene Ontology (GO) classification and functional enrichment were performed. GO covers three domains: biological process, cellular component, and molecular function. Functional enrichment was performed and the GO classification results between the WKY, SHR, and MA groups are shown in figure 4 a and b. Regarding biological processes, the categories “cellular process”,

“single-organism process”, “metabolic process”, and “biological regulation” showed large enrichment. The DEGs were involved in the “cell”, “cell part”, “organelle”, and “membrane”, according to their cellular component classification. In terms of the molecular functions, the “molecular transducer activity”, “binding”, “catalytic activity”, and “nucleic acid-binding transcription factor activity” showed large enrichment.

To further investigate the possible pathways affected directly by MA treatment in SHRs, DEGs were classified by performing KEGG pathway classification and functional enrichment. The terms with false discovery rates (FDRs) no larger than

0.01 are defined as being significantly enriched. As shown in figure 4 c and d, DEGs were found to be enriched in several signaling pathways, including “endocrine and metabolic diseases”, “neurodegenerative diseases”, “cardiovascular diseases”, “energy metabolism”, and “signaling molecules and interaction”.

Validation of the differentially expressed genes using real-time PCR

To further verify the reliability of the RNA-Seq data, real-time PCR was used to examine eight DEGs: *Angptl2, Erbb2, Klotho, Ednra, Ccr5, Gnb3, Gpr81*, and *Cyp1b1*. As shown in figure 5, trends in the expression data of the examined DEGs were the same as observed for RNA-Seq. Three genes, Angptl2, Erbb2, and Klotho, were downregulated in the SHR group but upregulated after the MA treatment. On the other hand, five genes, *Ednra, Ccr5, Gnb3, Gpr81* and *Cyp1b1* were upregulated in the SHR group but downregulated after MA treatment.

Discussion

Essential hypertension is a form of hypertension that accounts for the highest proportion of all hypertension cases[17]. Our results have shown that SBP and DBP were effectively reduced at 30–60 minutes after MA treatment, and a stable blood pressure reduction effect was obtained over continuous treatment for 7 days. This

research shows that acupuncture is effective and stable at lowering blood pressure, and this therapeutic effect is unique to the specific acupoint.

To reveal the central mechanism related to the management of blood pressure by acupuncture, PET-CT was used to explore the specific regulation of MA on the brain glucose metabolism of SHRs. The glucose metabolism of the PVH increased in the SHR group compared with the WKY group. After MA at KI3, the increased glucose metabolism of the PVH was significantly reversed, while the Sham-MA group showed no specific regulation of the metabolism of this brain area. Many human diseases, such as hypertension, obesity, and diabetes, are regulated by the PVH[18-20]. Additionally, the increased sympathetic outflow of the PVH and excessive activation of sympathetic synaptic N-methyl-D-aspartate receptors are essential for hypertension[21]. According to our PET-CT results, the PVH could be the target brain region for acupuncture at KI3 to regulate blood pressure. The pathological process associated with hypertension in the PVH is susceptible to acupuncture intervention. To further explain the effect of MA intervention on molecular modification in the PVH, a PVH transcriptome analysis was performed.

Our results showed that, according to the GO functional classification, the DEGs were enriched in the categories of “catalytic activity”, “transporter activity”, “molecular function regular”, and “signal transducer activity”. KEGG analysis revealed that the DEGs were involved in several pathways, including the “endocrine system”, “cardiovascular diseases”, and “neurodegenerative diseases”. Hypertension is associated with a reduction in key enzymes that maintain cardiac homeostasis, such as ALDH2[22-24]. However, the ability of these enzymes could be increased by enhanced catalytic activity to counteract the cytotoxic aldehydes produced by lipid peroxidation during hypertension[25] and improved ventricular dysfunction caused by hypertension[26]. One study showed that hypertension induced by angiotensin II increased the activation and abundance of transporters. The targeted therapy of transporters is important for the management of hypertension[27]. Therefore, improvements in catalytic activity and transporter activity may play an important role in the mechanism of MA intervention in hypertension.

The renin–angiotensin–aldosterone system (RAAS) is a complex endocrine system that regulates biological functions such as vasodilation and the contraction of blood vessels; it also tightly binds to the vasopressin system, endothelin, and the sympathetic nervous system. The activation of RASS is the basis upon which essential hypertension develops[28]. An increased level of angiotensin II can cause endothelial dysfunction and vascular remodeling during hypertension[29]. Therefore, we speculated that the effects of MA on the endocrine system, such as RAAS, may help to control high blood pressure in SHRs.

Upregulated DEGs in SHRs with MA

This study validated several DEGs that are upregulated after MA, including angiopoietin-like 2 (*Angptl2*), which encodes a secreted pro-inflammatory glycoprotein[30] that maintains tissue homeostasis by regulating blood pressure angiogenesis and inducing inflammation[31,32]. A decrease in circulating ANGPTL2 levels leads to an increase in systolic blood pressure in humans and mice. A decrease in blood pressure caused by the overexpression of *Angptl2* in mice indicated cardiac dysfunction accompanied by a decrease in Ca^{2+}-ATPase (SERCA) 2a signaling and a decrease in cardiac energy metabolism. In contrast, *Angptl2* knockdown increased

left ventricular contractility and blood pressure by AKT-SERCA2a signaling[33]. Therefore, these results indicate that increased levels of ANGPTL2 improve blood pressure.

Another upregulated DEG, *Klotho*—a newly discovered antiaging gene—encodes a transmembrane protein with an extracellular domain[34]. *Klotho* is mainly expressed in the brain and kidney[35,36]. Genetic *Klotho* defects lead to a premature aging phenotype, including a significantly shortened lifespan[37]. The circulating klotho level was found to be negatively correlated with age, and the prevalence of hypertension positively correlated with age[38]. The incidence of peroxide production and vascular disease in the kidneys increases in SHRs. The inhibition of NOX2 via the *Klotho* gene reduces the production of peroxides in the blood vessels and kidneys of SHRs and is the mechanism by which *Klotho* lowers blood pressure[39]. Additionally, another study showed that klotho protein complementation is involved in the inhibition of ANG signaling by binding to the ANG II type 1 receptor, ultimately inactivating the RAAS system[40]. Therefore, MA may exert its antihypertensive effect by increasing *Klotho* gene expression to inhibit oxidative stress and inactivate RAAS.

Together with neuregulin-1 (NRG-1), ERBB2—a subtype of the ERBB family—regulates many aspects of cardiovascular function, such as blood pressure and angiogenesis[41]. Inhibition of ERBB2 reduces the expression of NOS, thereby increasing blood pressure and heart rate by increasing sympathetic activity. NRG-1 lowers blood pressure by increasing NOS-mediated GABA[42,43]. Therefore, MA may induce NOS expression by increasing the levels of ERBB2, thereby inhibiting the sympathetic impulse to lower blood pressure in SHRs.

Downregulated DEGs in SHRs with MA

Endothelin receptor A (*Ednra*) encodes a G protein-coupled receptor that is an endogenous factor of vasoconstriction and is linked to endothelial dysfunction[44]. EDNRA binds to vasoconstrictors released by endothelial cells, and endothelin-1 (ET-1) increases blood vessel contraction and sodium retention, resulting in elevated blood pressure[45-47]. Increased EDNRA activity and elevated ET-1 levels have been found in the vascular system of hypertensive patients. The incidence of hypertension has been found to be significantly correlated with the expression of EDNRA ($p = 2.39 \times 10^{-4}$)[48]. This study found that the *Gpr81* gene played a role in cardiovascular control. The ET system is the primary mechanism by which GPR81 agonists induce vasoconstriction. Intense GPR81 agonism transmits stress signals in the tissues of the body, inducing the release of ET-1 that causes vasoconstriction[49]. Correspondingly, the expression level of EDNRA in SHRs was found to be downregulated after MA intervention, and the inactivation of GPR81 resulted in a decrease in ET-1 release, followed by a decrease in the binding of EDNRA to ET-1, which demonstrated that MA may play a role in relieving vasoconstriction and sodium retention through this pathway.

CCR5—a chemokine receptor—is expressed primarily on immune cells, such as T cells, natural killer cells, and monocytes. The recruitment of $CCR5^{+}$ immune cells has proven to be a prominent feature of many autoimmune diseases[50-52]. Hypertension is related to activation of the immune system and the development of an inflammatory response[53]. CCR5 expression was detected in the T cells of mice with hypertension, and high blood pressure was reduced by CCR5 antagonists. Additionally, no difference in systolic blood pressure was found between $CCR5^{-/-}$ and WT mice, suggesting that CCR5 may be a potential target for hypertension management[54]. Reactive oxygen species (ROS) production induced by CYP1B1 caused inflammation, cardiovascular hypertrophy, and endothelial dysfunction related to hypertension, mediated by the activation of

some signaling pathways, including ERK1/2 and c-SRC[55]. The increased activity of NADPH oxidase, p3MAPK and ROS production associated with ANG II-induced hypertension was alleviated in *Cyp1b1* knockout mice[56]. Therefore, a significant reduction in the expression levels of CCR5 and CYP1B1 after MA intervention in SHRs confirmed that MA has the effect of reducing inflammation in hypertension.

The G protein β3 (GNB3) subunit is involved in G protein-coupled receptor signal transduction. Polymorphisms of GNB3 are related to some diseases, such as hypertension, obesity, and diabetes. However, the pathogenesis of GNB3 in these diseases remains uncharacterized[57]. The *Gnb3* C825T polymorphism is a marker for the treatment of hypertension, with a phenotype featuring enhanced sodium-proton reverse motility activity. Increased essential hypertension is related to the T allele of the *Gnb3* C825T polymorphism[58]. Therefore, MA intervention may regulate hypertension by downregulating GNB3 and inactivating the T allele of the *Gnb3* C825T polymorphism.

Conclusion

Our data suggest that repeated MA treatment of acupoint KI3 reduces the elevated blood pressure of SHRs. PET-CT scanning results further indicated that PVH could be the target brain area for MA at KI3 to manage blood pressure. Furthermore, whole transcriptome sequencing of PVH was used to explore how DEGs regulated by acupuncture in SHRs are related to neurodegenerative diseases, cardiovascular diseases, and immune system signaling pathways, thereby providing a theoretical basis for the further study of acupuncture treatment in hypertension.

Methods

Experimental Animals

Male SHRs and WKY rats (15 weeks old), purchased from Beijing Vital River Laboratory Animal Technology Co., Ltd (Beijing, China), had free access to food and water under room temperature 20–22 ℃ and a 12 h light/12 h dark cycle.

All animals were handled in accordance with the People's Republic of China Ministry of Science and Technology Laboratory Animal Care guidelines and the experiment was approved by the Experimental Animal Ethics Committee of Guangzhou University of Chinese Medicine (ref. S2017003).

Groups and Acupuncture Treatment

WKY rats were used as the controls (WKY, n = 10). SHRs were randomly assigned into three groups: SHRs (SHR, n = 10), SHRs with manual acupuncture (MA) treatment at acupoint KI3 (MA, n = 10), and SHRs receiving sham-MA treatment (sham-MA, n = 10). The position of the sham acupoint was selected as the space between the 3rd and 4th toes on the back of the foot. The MA treatment and sham-MA treatment was performed according to a previous study[12]. MA and sham-MA groups received acupuncture for 7 consecutive days for 10 minutes per day.

Blood Pressure Measurement

Systolic blood pressure (SBP) and diastolic blood pressure (DBP) were measured with a blood pressure monitor (CODA7m, Kent Scientific Corporation, Torrington, Connecticut, USA), according to the method described previously[12], at 30, 60, and 90 min after the first day of therapy, or 30 min after each day's acupuncture treatment in the 7 day therapy.

PET-CT Scanning

All PET-CT scans were performed on the animal molecular imaging research platform of Sun Yat-sen Medical College. After receiving acupuncture therapy, all rats were injected intravenously with 1.5 mci/kg ^{18}F-FDG, followed by PET-CT scanning. After the FDG-PET image was acquired, it was reconstructed through a 128 × 128 × 159 matrix and filtered projection.

After the PET-CT scan, all rats were anesthetized and sacrificed by intraperitoneal injection of 30 mg/kg sodium pentobarbital.

Tissue Processing

The PVHs that were used for RNA-Seq analysis were the WKY, SHR, and MA groups, because no significant difference was found in reducing BP between the SHR and sham-MA groups. At 24 hours after the 7 day treatment, the rats were anesthetized and killed, and the PVH was rapidly removed. The total RNA was extracted from the PVH by using the RNeasy Mini Kit (74104, Qiagen, Beijing, China), according to the manufacturer's protocol, and an Agilent 2100 Bioanalyzer (Agilent RNA 6000 Nano Kit) was used to perform quality control for the total RNA.

RNA-Seq Analysis

Transcriptome sequencing was performed with BGI Co., Ltd., Shenzhen, China (http://www.genomics.cn/). Briefly, DNA libraries were constructed using the TruSeq stranded mRNA library preparation kit (Illumina, San Diego, CA, USA) according to the manufacturer's instructions. Paired-end reads of 100 bp were read, and the DNA libraries were sequenced on the BGISEQ-500 platform for sequence data analysis.

Quality Control for Raw Data

The raw data for sequencing included low-quality, adaptor-polluted material, with a high content of unknown base (N) reads. These reads needed to be removed before data analysis to ensure the reliability of the results. The Q20, Q30, and clean read ratios were calculated, and subsequent analyses were based on these clean reads.

Differential Expression Analysis

Clean reads were mapped to the reference using Bowtie2[59], and the gene expression level was calculated with RSEM[60]. DEGs with DEseq2 were detected as requested[61]. DEGs were chosen according to the parameters with a fold change ≥ 2 and an adjusted p-value ($p \leq 0.05$). Then, the Pearson correlation between all samples was calculated using cor, and hierarchical clustering between all samples was performed using hclust. Gene expression was compared between SHRs and WKYs, and between MA and SHR groups. The overlap in upregulated and downregulated gene expression between the different groups was analyzed using BioVenn[62]. GO and KEGG classification and functional enrichment were performed for all identified DEGs.

Real-Time PCR

Eight DEGs were selected for validation using qRT-PCR. cDNA was produced from hypothalamus mRNA (2 μg) using an Invitrogen™ SuperScript™ II Reverse Transcriptase reagent kit (Takara, Shanghai, China). OneStep RT-PCR Enzyme mix (Qiagen, Beijing, China) was used to for qRT-PCR on an ABI ViiA 7 PCR System (Thermo Fisher Scientific, USA). The Ct value in the reaction was collected using a corrected threshold setting. β-αctin was used as the internal reference gene to confirm gene expression levels, and the relative quantification was determined using the $2^{-\Delta\Delta Ct}$ method. The primers used for qRT-PCR validation are shown in supplementary table 1.

Statistical Analysis

All data were analyzed using a one-way analysis of variance test via SPSS 17.0 (SPSS Inc., Chicago, USA). An LSD post hoc test was used to determine the group differences. Data were expressed as the mean ± SD, and $p < 0.05$ was considered statistically significant.

Declarations

ETHICS STATEMENT

Animal procedures were approved by the Ethics Committee of the Guangzhou University of Chinese Medicine.

AUTHOR CONTRIBUTIONS

X. S. L. designed the research. J. L. wrote the manuscript. J. L., C. P., Z. M. Z., C. Y. L., Y. J. F. and D. J. L. prepared the materials and performed the experiments. D. H. L., C. P. and X. S. L. analyzed the data. All authors read and approved the final manuscript.

FUNDING

This work was supported by the National Natural Science Foundation of China (ref. 81473600).

ACKONWLEDGMENTS

We thank the Lingnan Medical Research Center for their substantial facilitations of all necessary materials and equipment.

CONFLICTS OF INTEREST

The authors declare that they have no conflict of interest.

References

1. Nijskens, C. M., Veldkamp, S. R., Van Der Werf, D. J., Boonstra, A. H. & Ten Wolde, M. Funduscopy: Yes or no? Hypertensive emergencies and retinopathy in the emergency care setting; a retrospective cohort study. *The Journal of Clinical Hypertension* (2020).
2. James, P. A. *et al.* 2014 evidence-based guideline for the management of high blood pressure in adults: report from the panel members appointed to the Eighth Joint National Committee (JNC 8). *Jama***311**, 507-

520 (2014).

3. Lim, S. S. *et al.* A comparative risk assessment of burden of disease and injury attributable to 67 risk factors and risk factor clusters in 21 regions, 1990–2010: a systematic analysis for the Global Burden of Disease Study 2010. *The lancet***380**, 2224-2260 (2012).
4. Poulter, N. R., Prabhakaran, D. & Caulfield, M. Hypertension. *Lancet***386**, 801-812 (2015).
5. Steubl, D. *et al.* Association of Serum Uromodulin with Death, Cardiovascular Events, and Kidney Failure in CKD. *Clinical Journal of the American Society of Nephrology***15**, 616-624 (2020).
6. Wu, X. *et al.* Value of a Machine Learning Approach for Predicting Clinical Outcomes in Young Patients With Hypertension. *Hypertension***75**, 1271-1278 (2020).
7. Palmer, B. F. Hypertension management in patients with chronic kidney disease. *Current hypertension reports***10**, 367-373 (2008).
8. Xin, J.-J. *et al.* Antihypertensive and Antifibrosis Effects of Acupuncture at PC6 Acupoints in Spontaneously Hypertensive Rats and the Underlying Mechanisms. *Frontiers in Physiology***11** (2020).
9. Hong, S., Ahn, L., Kwon, J. & Choi, D.-j. Acupuncture for Regulating Blood Pressure of Stroke Patients: A Systematic Review and Meta-Analysis. *The Journal of Alternative and Complementary Medicine* (2020).
10. Zhang, J. *et al.* Acupuncture at LR3 and KI3 shows a control effect on essential hypertension and targeted action on cerebral regions related to blood pressure regulation: a resting state functional magnetic resonance imaging study. *Acupuncture in Medicine*, 0964528420920282 (2020).
11. Li, J. *et al.* Changes in cerebral glucose metabolism after acupuncture at KI3 in spontaneously hypertensive rats: a positron emission tomography study. *Acupuncture in Medicine***37**, 107-115 (2019).
12. Li, J. *et al.* Effect of acupuncture at LR3 on cerebral glucose metabolism in a rat model of hypertension: a 18F-FDG-PET study. *Evidence-Based Complementary and Alternative Medicine***2018** (2018).
13. Zhu, Q. *et al.* Neuroendocrine regulation of energy metabolism involving different types of adipose tissues. *International journal of molecular sciences***20**, 2707 (2019).
14. Maekawa, S., Wang, P.-C. & Chen, S.-C. Comparative study of immune reaction against bacterial infection from transcriptome analysis. *Frontiers in immunology***10**, 153 (2019).
15. Yu, W. *et al.* Molecular-level effects of acupuncture on depression: a genome-wide transcriptome analysis of pituitary gland in rats exposed to chronic restraint stress. *Journal of Traditional Chinese Medicine***37**, 486-495 (2017).
16. Garcia-Vivas, J. M. *et al.* Transcriptomic profiling of adipose tissue in obese women in response to acupuncture catgut embedding therapy with moxibustion. *The Journal of Alternative and Complementary Medicine***22**, 658-668 (2016).
17. McBryde, F. D., Hart, E. C., Ramchandra, R. & Paton, J. F. Evaluating the carotid bodies and renal nerves as therapeutic targets for hypertension. *Autonomic Neuroscience***204**, 126-130 (2017).
18. Qin, C., Li, J. & Tang, K. The Paraventricular Nucleus of the Hypothalamus: Development, Function, and Human Diseases. *Endocrinology***159**, 3458 (2018).
19. Kim, E. R. *et al.* Paraventricular hypothalamus mediates diurnal rhythm of metabolism. *Nature communications***11**, 1-17 (2020).
20. Tuttolomondo, A. *et al.* Endothelial Function, Adipokine Serum Levels, and White Matter Hyperintesities in Subjects With Diabetic Foot Syndrome. *The Journal of Clinical Endocrinology & Metabolism***104**, 3920-3930

(2019).

21. Ma, H., Chen, S. R., Chen, H. & Pan, H. L. Endogenous AT1 receptor–protein kinase C activity in the hypothalamus augments glutamatergic input and sympathetic outflow in hypertension. *The Journal of physiology* (2019).
22. Shimizu, Y. *et al.* Potential mechanisms underlying the association between single nucleotide polymorphism (BRAP and ALDH2) and hypertension among elderly Japanese population. *Scientific Reports***10**, 1-9 (2020).
23. Zheng, Y. *et al.* Association Between ALDH-2 rs671 and Essential Hypertension Risk or Blood Pressure Levels: A Systematic Review and Meta-Analysis. *Frontiers in Genetics***11** (2020).
24. Mei, X.-F. *et al.* ALDH2 Gene rs671 Polymorphism May Decrease the Risk of Essential Hypertension. *International Heart Journal*, 19-259 (2020).
25. Backos, D. S., Fritz, K. S., Roede, J. R., Petersen, D. R. & Franklin, C. C. Posttranslational modification and regulation of glutamate–cysteine ligase by the α,β-unsaturated aldehyde 4-hydroxy-2-nonenal. *Free Radical Biology & Medicine***50**, 14-26 (2011).
26. Campos, J. C. *et al.* Increased clearance of reactive aldehydes and damaged proteins in hypertension-induced compensated cardiac hypertrophy: impact of exercise training. *Oxidative medicine and cellular longevity***2015** (2015).
27. Nguyen, M. T., Lee, D. H., Delpire, E. & Mcdonough, A. A. Differential regulation of Na+ transporters along nephron during ANG II-dependent hypertension: distal stimulation counteracted by proximal inhibition. *Am J Physiol Renal Physiol***305**, F510-F519 (2013).
28. Emdin, M. *et al.* Biomarkers of activation of renin-angiotensin-aldosterone system in heart failure: how useful, how feasible? *Clinica Chimica Acta***443**, 85-93 (2015).
29. Yan, X. *et al.* Gallic acid attenuates angiotensin II-induced hypertension and vascular dysfunction by inhibiting the degradation of endothelial nitric oxide synthase. *Frontiers in pharmacology***11**, 1121 (2020).
30. Desjardins, M.-P. *et al.* Levels of angiopoietin-like-2 are positively associated with aortic stiffness and mortality after kidney transplantation. *American Journal of Hypertension***30**, 409-416 (2017).
31. Kenawy, M. Z., Sabry, J. H., Akl, E. M. & Emam, N. A. Angiopoietin-like protein 2 in psoriasis: a new linkage with metabolic syndrome. *Advances in Dermatology and Allergology/Post□py Dermatologii i Alergologii***37**, 86 (2020).
32. Xiang, H. *et al.* Knockdown of ANGPTL2 Protects Renal Tubular Epithelial Cells Against Hypoxia/Reoxygenation-Induced Injury via Suppressing TLR4/NF-κB Signaling Pathway and Activating Nrf2/HO-1 Signaling Pathway. *Cell Transplantation***29**, 0963689720946663 (2020).
33. Tian, Z. *et al.* ANGPTL2 activity in cardiac pathologies accelerates heart failure by perturbing cardiac function and energy metabolism. *Nature Communications***7**, 13016 (2016).
34. Peshes-Yeloz, N. *et al.* Role of Klotho protein in tumor genesis, cancer progression, and prognosis in patients with high-grade glioma. *World neurosurgery***130**, e324-e332 (2019).
35. Kale, A., Sankrityayan, H., Anders, H.-J. & Gaikwad, A. B. Epigenetic and non-epigenetic regulation of Klotho in kidney disease. *Life Sciences*, 118644 (2020).
36. Kan, W.-C. *et al.* Effect of osthole on advanced glycation end products-induced renal tubular hypertrophy and role of klotho in its mechanism of action. *Phytomedicine***53**, 205-212 (2019).

37. Singh, A. P. *et al.* αKlotho Regulates Age-Associated Vascular Calcification and Lifespan in Zebrafish. *Cell reports***28**, 2767-2776. e2765 (2019).
38. Joffres, M. *et al.* Hypertension prevalence, awareness, treatment and control in national surveys from England, the USA and Canada, and correlation with stroke and ischaemic heart disease mortality: a cross-sectional study. *BMJ open***3**, e003423 (2013).
39. Yuhong, W. & Zhongjie, S. Klotho gene delivery prevents the progression of spontaneous hypertension and renal damage. *Hypertension***54**, 810 (2009).
40. Takenaka, T. *et al.* Klotho Ameliorates Medullary Fibrosis and Pressure Natriuresis in Hypertensive Rat Kidneys. *Hypertension***72**, 1151-1159 (2018).
41. Oghenerukevwe, O., Hill, M. F. & Sawyer, D. B. Neuregulin in cardiovascular development and disease. *Circulation Research***111**, 1376-1385 (2012).
42. Matsukawa, R., Hirooka, Y., Ito, K. & Sunagawa, K. Inhibition of neuregulin-1/ErbB signaling in the rostral ventrolateral medulla leads to hypertension through reduced nitric oxide synthesis. *American journal of hypertension***26**, 51-57 (2013).
43. Kim, H. S., Cho, J. W., Hidaka, K. & Morisaki, T. Activation of MEK–ERK by heregulin-β1 promotes the development of cardiomyocytes derived from ES cells. *Biochemical and biophysical research communications***361**, 732-738 (2007).
44. Liu, F. *et al.* Associations of endothelial system genes with blood pressure changes and hypertension incidence: the gensalt study. *American journal of hypertension***28**, 780-788 (2014).
45. A Khalil, R. Modulators of the vascular endothelin receptor in blood pressure regulation and hypertension. *Current molecular pharmacology***4**, 176-186 (2011).
46. Mazzuca, M. Q. & Khalil, R. A. Vascular endothelin receptor type B: structure, function and dysregulation in vascular disease. *Biochemical pharmacology***84**, 147-162 (2012).
47. Vercauteren, M. *et al.* Endothelin ETA receptor blockade, by activating ETB receptors, increases vascular permeability and induces exaggerated fluid retention. *Journal of Pharmacology and Experimental Therapeutics***361**, 322-333 (2017).
48. Liu, F. *et al.* Associations of Endothelial System Genes With Blood Pressure Changes and Hypertension Incidence: The GenSalt Study. *American Journal of Hypertension***28**, 780 (2015).
49. Allcock, G. H., Warner, T. D. & Vane, J. R. Roles of endothelin receptors in the regional and systemic vascular responses to ET-1 in the anaesthetized ganglion-blocked rat: use of selective antagonists. *British journal of pharmacology***116**, 2482-2486 (1995).
50. Godoy, G. J. *et al.* Differences in T regulatory cells between mouse strains frequently used in immunological research: Treg cell quantities and subpopulations in NOD, B6 and BALB/c mice. *Immunology Letters* (2020).
51. He, J. *et al.* Blocking Matrix Metalloproteinase-9 Abrogates Collagen-Induced Arthritis via Inhibiting Dendritic Cell Migration. *The Journal of Immunology***201**, 3514-3523 (2018).
52. Reuveni, D. *et al.* The critical role of chemokine (c–c Motif) receptor 2-Positive Monocytes in autoimmune cholangitis. *Frontiers in immunology***9**, 1852 (2018).
53. Mettimano, M. *et al.* Blood pressure regulation by CCR genes. *Clinical & Experimental Hypertension***28**, 611 (2006).

54. Krebs, C. *et al.* CCR5 deficiency does not reduce hypertensive end-organ damage in mice. *American journal of hypertension***25**, 479-486 (2012).
55. Aurelie, N. D. C. & Touyz, R. M. Cell signaling of angiotensin II on vascular tone: novel mechanisms. *Current Hypertension Reports***13**, 122-128 (2011).
56. Jennings, B. L. *et al.* Involvement of cytochrome P-450 1B1 in renal dysfunction, injury, and inflammation associated with angiotensin II-induced hypertension in rats. *Ajp Renal Physiology***302**, F408-420 (2012).
57. Ye, Y. *et al.* Ablation of the GNB3 gene in mice does not affect body weight, metabolism or blood pressure, but causes bradycardia. *Cellular Signalling***26**, 2514-2520 (2014).
58. Klenke, S., Kussmann, M. & Siffert, W. The GNB3 C825T polymorphism as a pharmacogenetic marker in the treatment of hypertension, obesity, and depression. *Pharmacogenetics & Genomics***21**, 594 (2011).
59. Langmead, B. & Salzberg, S. L. Fast gapped-read alignment with Bowtie 2. *Nature methods***9**, 357 (2012).
60. Li, B. & Dewey, C. N. RSEM: accurate transcript quantification from RNA-Seq data with or without a reference genome. *BMC bioinformatics***12**, 323 (2011).
61. Love, M. I., Huber, W. & Anders, S. Moderated estimation of fold change and dispersion for RNA-seq data with DESeq2. *Genome biology***15**, 550 (2014).
62. Zheng, R. *et al.* Transcriptomic Insights into the Response of the Olfactory Bulb to Selenium Treatment in a Mouse Model of Alzheimer's Disease. *International Journal of Molecular Sciences***20**, 2998 (2019).

Tables

Table 1. Changes in brain glucose metabolism in the SHR group versus the WKY group.

		Peak coordinates(mm)		
Anatomical	**Max_T**	**X**	**Y**	**Z**
Increased cerebral glucose metabolism				
Agranular insular cortex	4.9318	-3.5204	5.4957	2.7121
Accumbens nucleus	5.2113	-1.4854	5.8600	3.4421
Hypothalamus	5.2084	5.2113	3.7700	-5.1579
Infralimbic cortex	5.8891	-1.7353	4.5220	3.6721
Lateral orbital cortex	6.1112	-2.0434	4.2133	4.4821
Medial orbital cortex	4.4363	-0.8938	3.6557	5.9021
Olfactory bulb	5.1011	-0.9170	3.4705	7.7521
Thalamus	7.7016	-2.1748	6.3023	-3.2279
Ventral orbital cortex	6.5624	-1.9962	3.8448	4.1621
Dorsal thalamus lateral nucleus group	7.7298	-2.2315	6.2336	-3.8979
Dorsal thalamus	7.7298	-2.2315	6.2336	-3.8979
Insular cortex	5.3416	-3.8877	5.3742	2.4321
Nucleus around the septal area	5.3113	-1.2554	5.8800	3.3821
Orbital cortex	6.2724	-1.3262	4.5648	4.7821
Retrosplenial cortex	5.5247	0.9280	2.1260	-5.9179
Decreased cerebral glucose metabolism				
Cingulate cortex	5.4028	-0.4106	0.8324	2.8521
Cingulate gyrus	5.8715	-0.8600	0.4552	2.4821
Motor cortex	6.7750	1.3706	-0.1732	-2.6879
Sensory cortex	6.4710	3.2213	0.4987	-0.6379
Visual cortex	5.8175	5.7482	2.5629	-5.5579

Table 2. Changes in brain glucose metabolism in the MA group versus the SHR group.

		Peak coordinates(mm)		
Anatomical	**Max_T**	**X**	**Y**	**Z**
Increased cerebral glucose metabolism				
Cerebellum posterior lobe	3.9995	3.6906	5.0247	-10.8638
Visual cortex	5.0153	2.8525	0.9995	-9.0979
Decreased cerebral glucose metabolism				
Accumbens nucleus	5.0146	-2.1170	5.5260	2.3221
Hypothalamus	4.0081	0.7951	7.9986	-1.9379
Olfactory bulb	6.1332	-1.0071	3.6408	6.1621
Prefrontal cortex	5.5397	-1.1074	4.0621	5.9221
Thalamus	4.5132	-2.1388	5.8601	-3.0379
Anterior commissure	5.1151	-0.8343	4.2171	6.1621
Dorsal thalamus	4.1132	-1.9388	6.5601	-2.9379
Hypothalamus tuberal region	3.8469	0.9891	8.3124	-2.3779
Orbital cortex	5.0835	-0.8844	3.3049	5.8421
Striatum	4.2395	-2.7483	6.1624	1.9821

Table 3. Changes in brain glucose metabolism in the Sham-MA group versus the SHR group.

		Peak coordinates(mm)		
Anatomical	**Max_T**	**X**	**Y**	**Z**
Increased cerebral glucose metabolism				
Medulla oblongata	6.6063	-1.6222	7.9011	-11.9179
Decreased cerebral glucose metabolism				
Anterior olfactory nucleus	6.5951	-1.1251	6.0005	3.2421
Accumbens nucleus	8.8591	-1.4525	5.7490	2.2221
Basal ganglia	6.4873	-1.6531	5.2821	2.7621
Caudate putamen	6.4873	-1.6531	5.2821	2.7621
Olfactory bulb	6.0483	-1.4155	3.7857	6.8621
Prefrontal cortex	7.0097	-1.1187	5.8147	2.9421
Anterior commissure	6.9999	-1.7768	6.5065	2.0421
Nucleus around the septal area	8.3091	-1.5325	5.8849	2.4421
Orbital cortex	5.9403	-1.5326	4.7666	3.7221

Figures

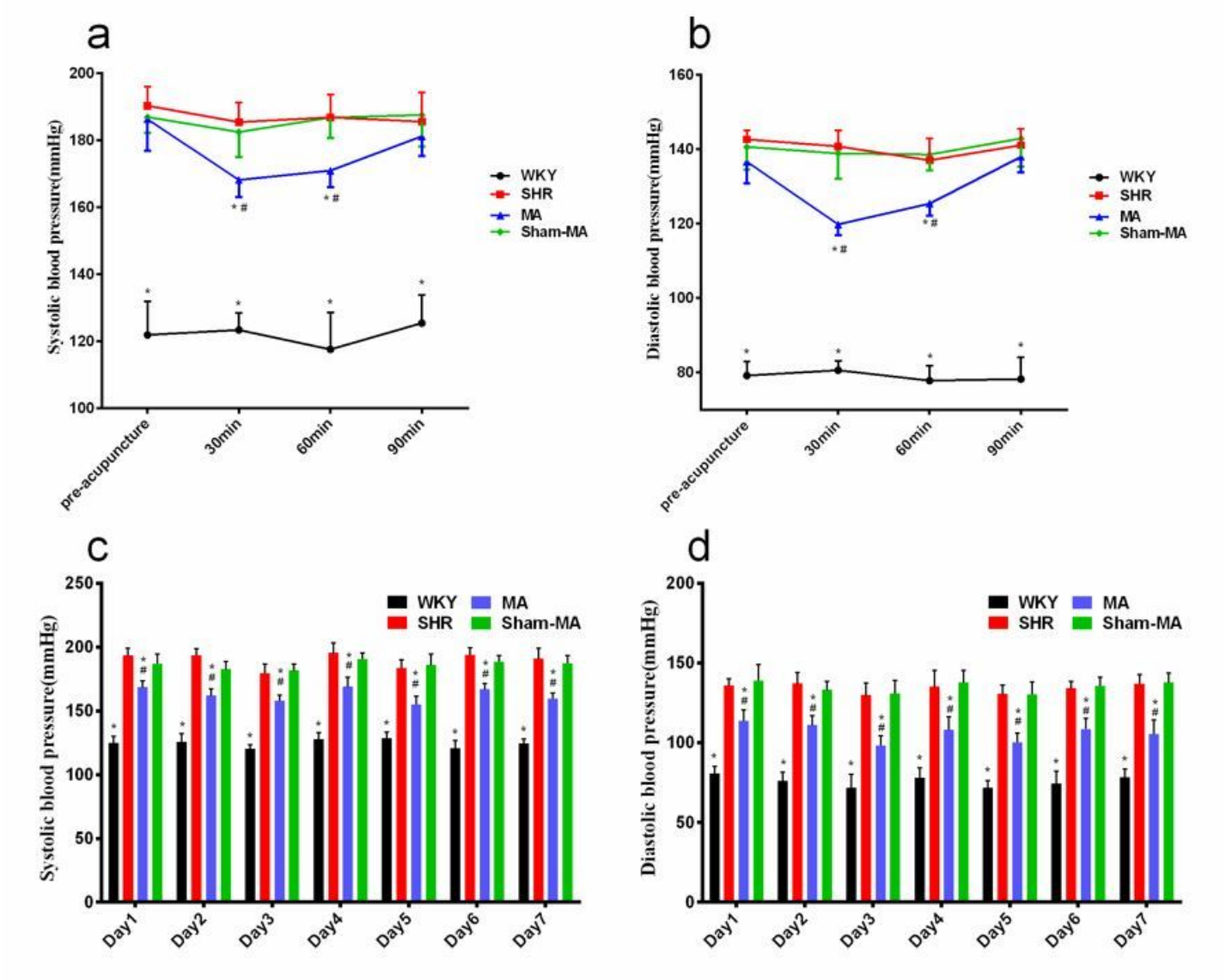

Figure 1

Reducing blood pressure (BP) effects induced by MA in SHRs. (a and c) Differences in systolic blood pressure (SBP) and (b and d) diastolic blood pressure (DBP) among WKY, SHR, MA and Sham-MA groups were detected at 30, 60 and 90 min after the first day of treatment, or every day of the 7 day treatment. * $p < 0.05$ versus the SHR group, # $p < 0.05$ versus the Sham-MA group.

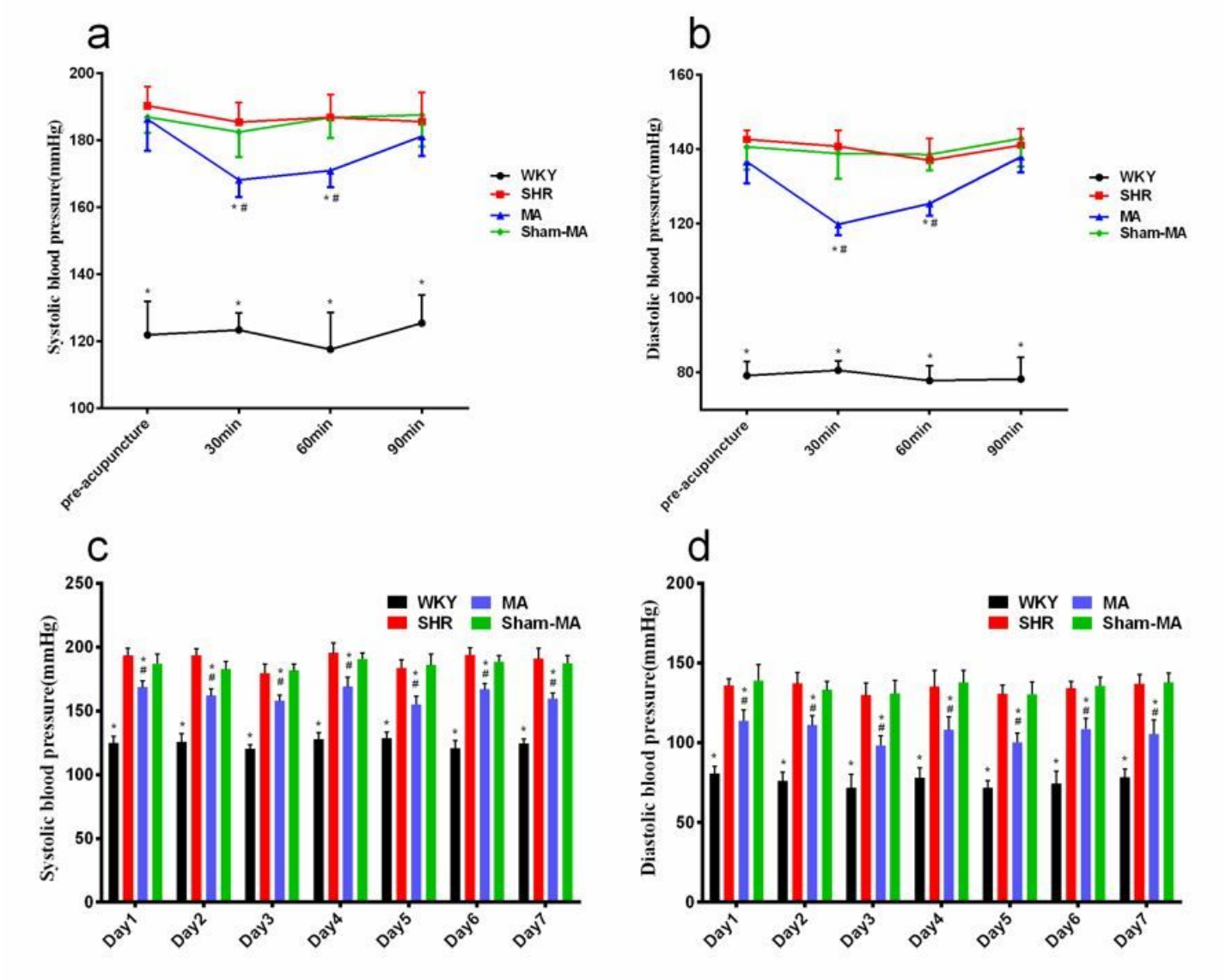

Figure 1

Reducing blood pressure (BP) effects induced by MA in SHRs. (a and c) Differences in systolic blood pressure (SBP) and (b and d) diastolic blood pressure (DBP) among WKY, SHR, MA and Sham-MA groups were detected at 30, 60 and 90 min after the first day of treatment, or every day of the 7 day treatment. * $p < 0.05$ versus the SHR group, # $p < 0.05$ versus the Sham-MA group.

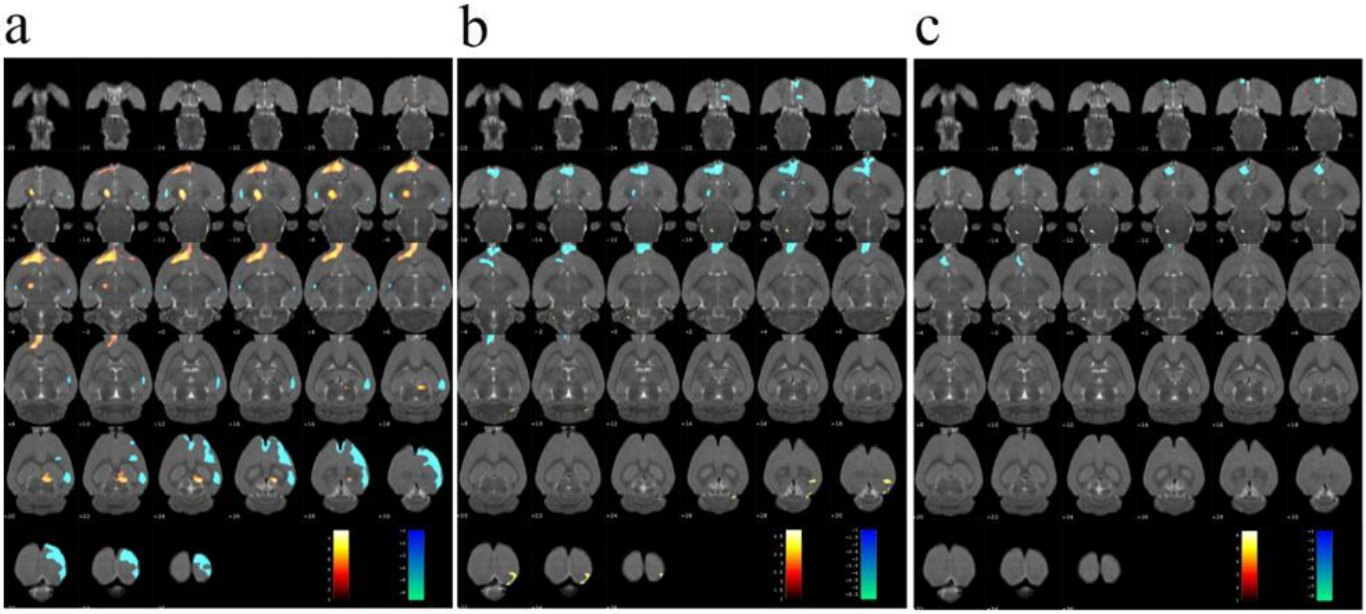

Figure 2

Changes of glucose metabolism in the rat brain. Regional glucose metabolism was scanned after the 7 day treatment. Results are overlaid on an axial view of the rat brain and mapped to the Paxinos and Watson rat brain atlas. (a) SHR group versus WKY group, (b) MA group versus SHR group, (c) Sham-MA group versus SHR group. Color bars represent the t-value of each significant voxel.

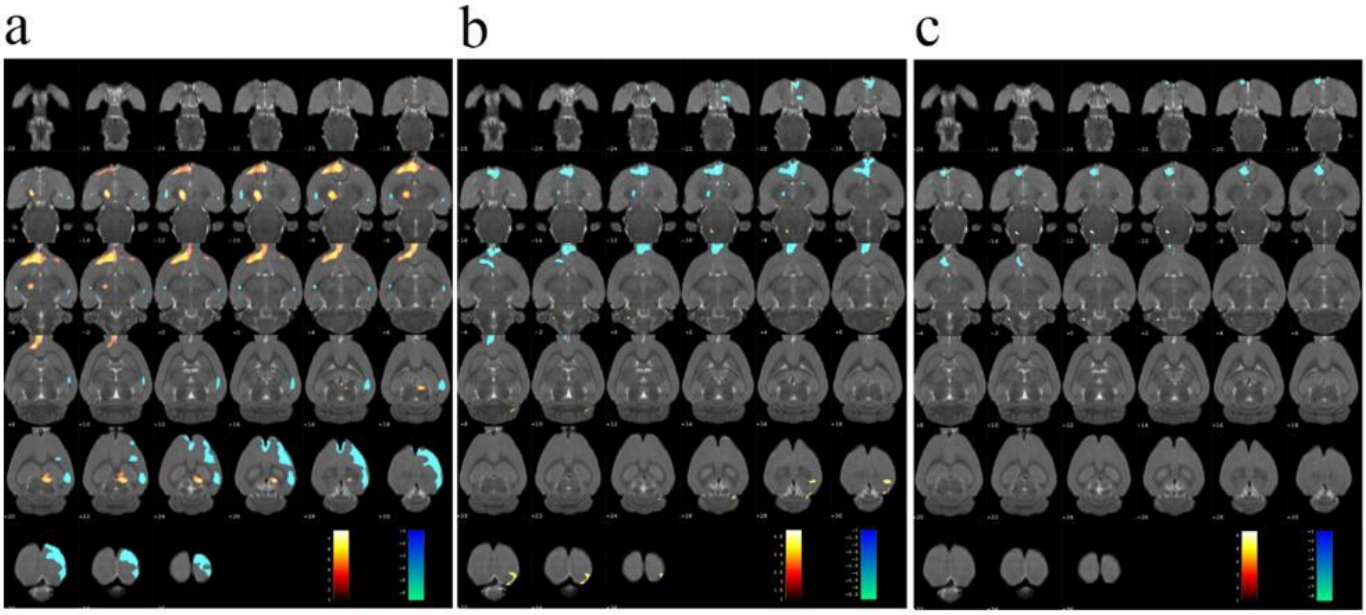

Figure 2

Changes of glucose metabolism in the rat brain. Regional glucose metabolism was scanned after the 7 day treatment. Results are overlaid on an axial view of the rat brain and mapped to the Paxinos and Watson rat brain

atlas. (a) SHR group versus WKY group, (b) MA group versus SHR group, (c) Sham-MA group versus SHR group. Color bars represent the t-value of each significant voxel.

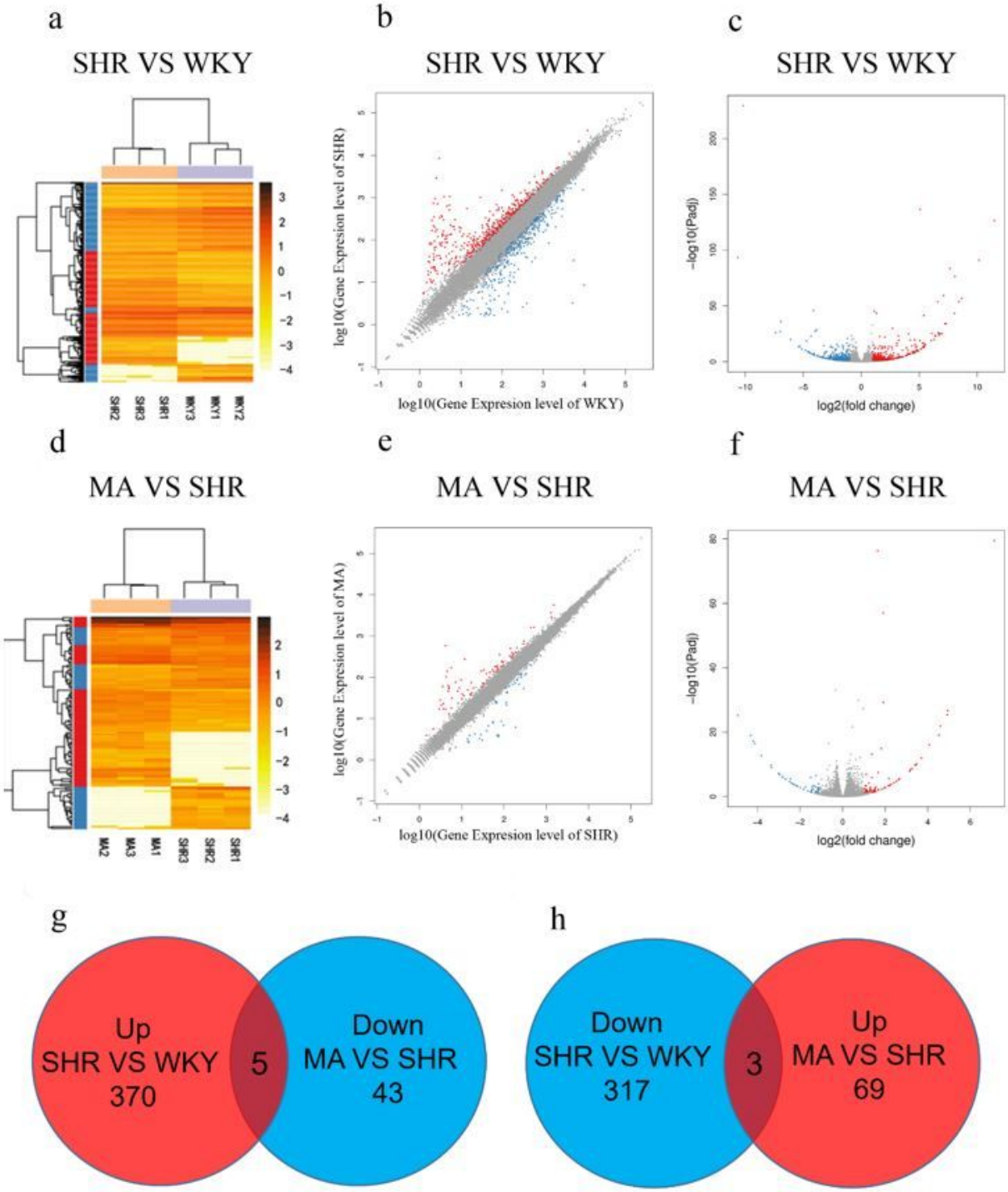

Figure 3

Significantly different mRNA expression in the PVH of WKY, SHR, and MA. The hierarchical clustering (a and d), scatter plot (b and e), and volcano plot (c and f) show differentially expressed genes (DEGs) between the WKY, SHR, and MA groups with the red and blue colors, respectively suggesting upregulated or downregulated expression; (g and h) Venn diagrams of the overlapping DEGs between the groups are shown. Five genes

increased in the SHR group but decreased in the MA group. Three genes decreased in the SHR group but increased in the MA group.

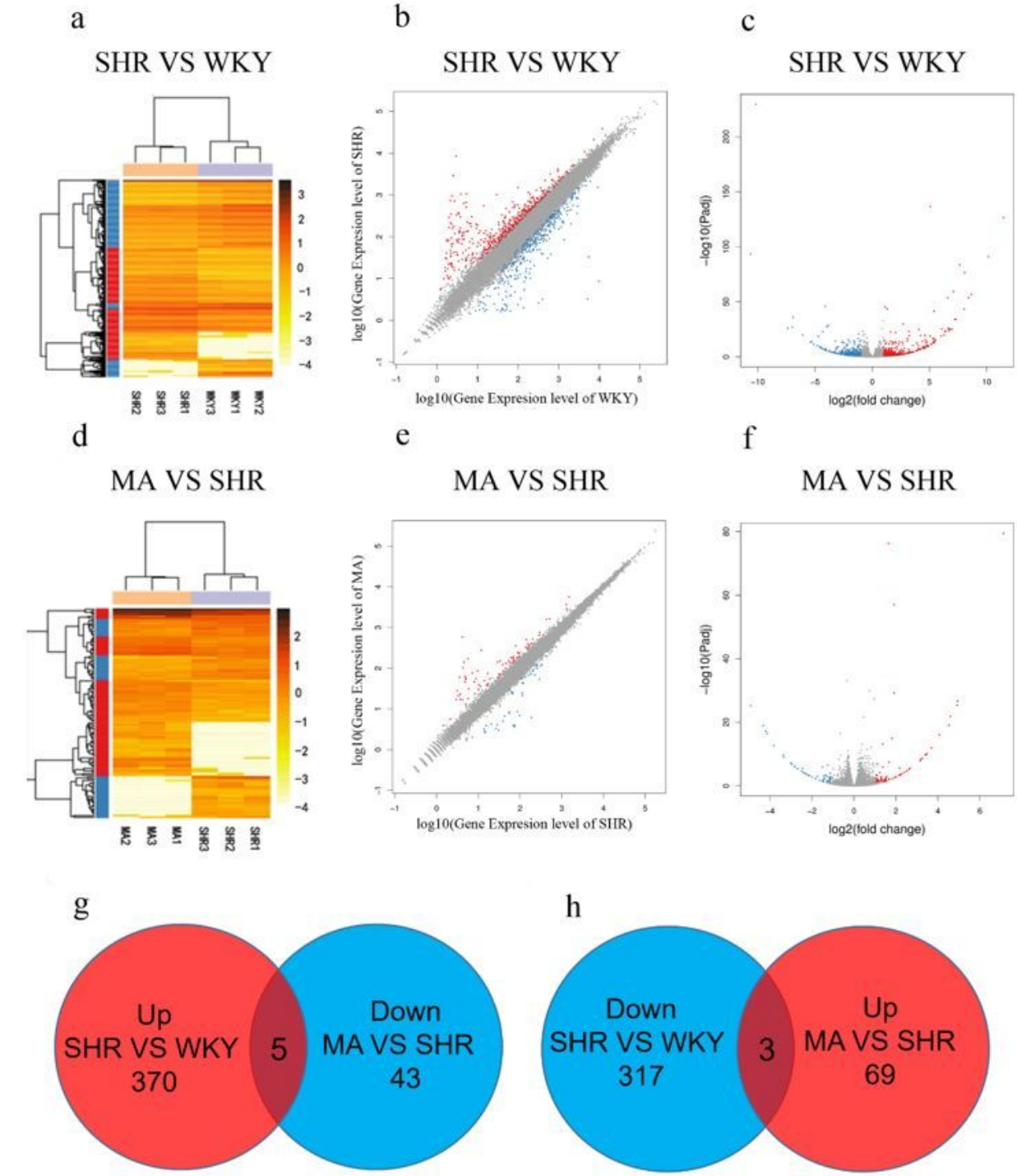

Figure 3

Significantly different mRNA expression in the PVH of WKY, SHR, and MA. The hierarchical clustering (a and d), scatter plot (b and e), and volcano plot (c and f) show differentially expressed genes (DEGs) between the WKY, SHR, and MA groups with the red and blue colors, respectively suggesting upregulated or downregulated expression; (g and h) Venn diagrams of the overlapping DEGs between the groups are shown. Five genes

increased in the SHR group but decreased in the MA group. Three genes decreased in the SHR group but increased in the MA group.

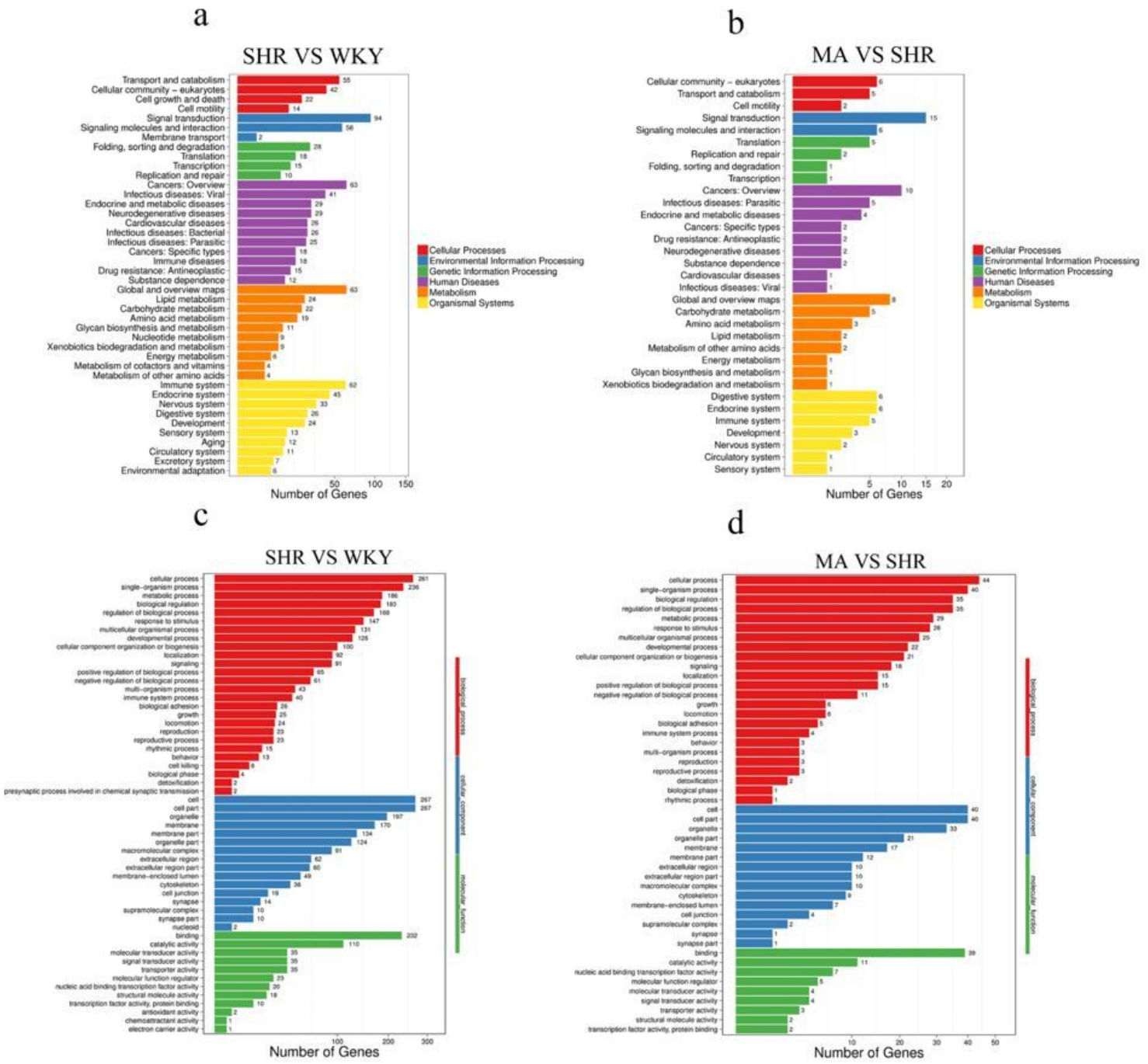

Figure 4

The DEG number of the most enriched Gene Ontology (GO) terms(a and b) and KEGG Pathway functional enrichment results(c and d) for the DEGs between WKY, SHR, and MA. (a and c) SHR versus WKY; (b and d) MA versus SHR.

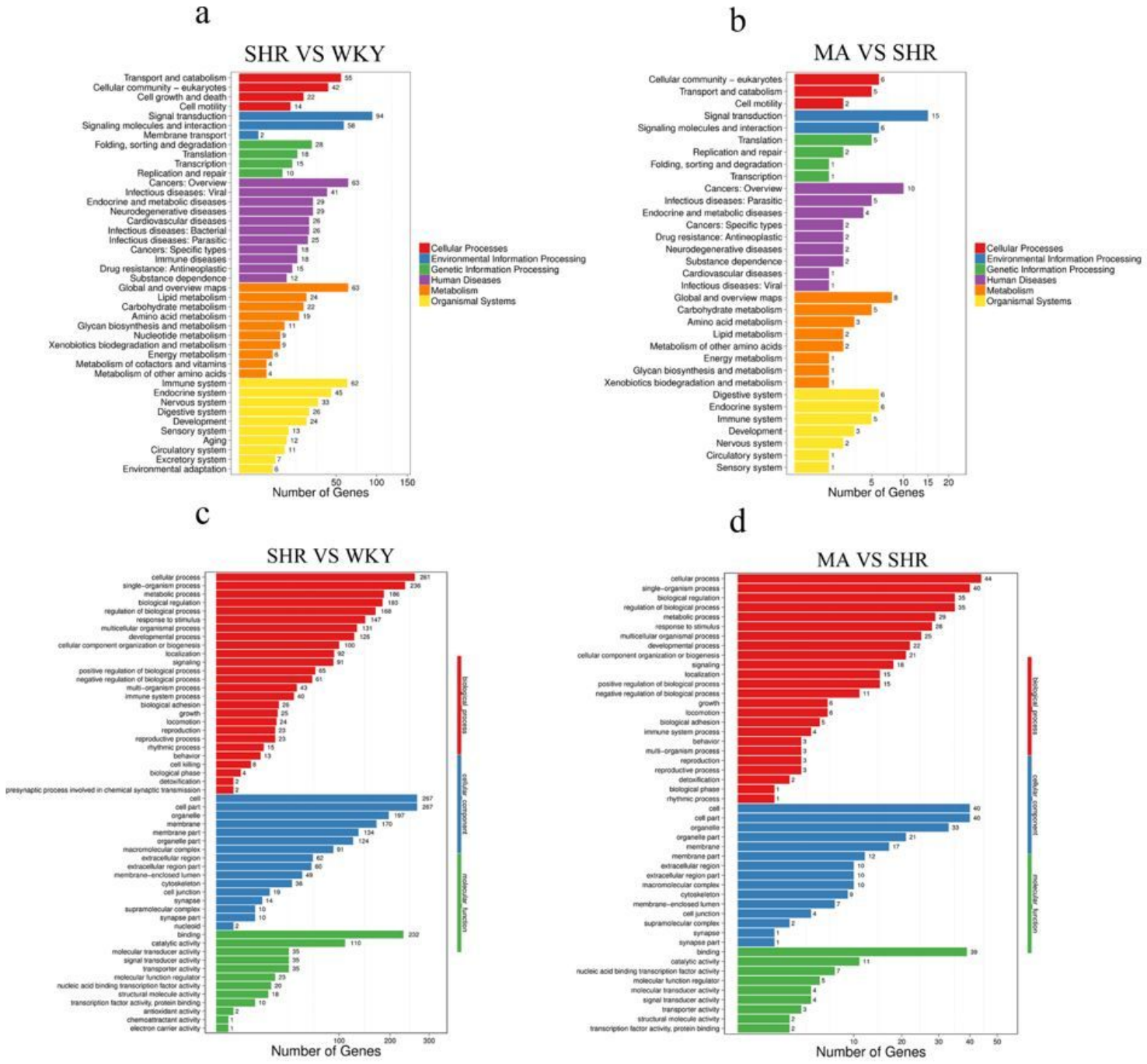

Figure 4

The DEG number of the most enriched Gene Ontology (GO) terms(a and b) and KEGG Pathway functional enrichment results(c and d) for the DEGs between WKY, SHR, and MA. (a and c) SHR versus WKY; (b and d) MA versus SHR.

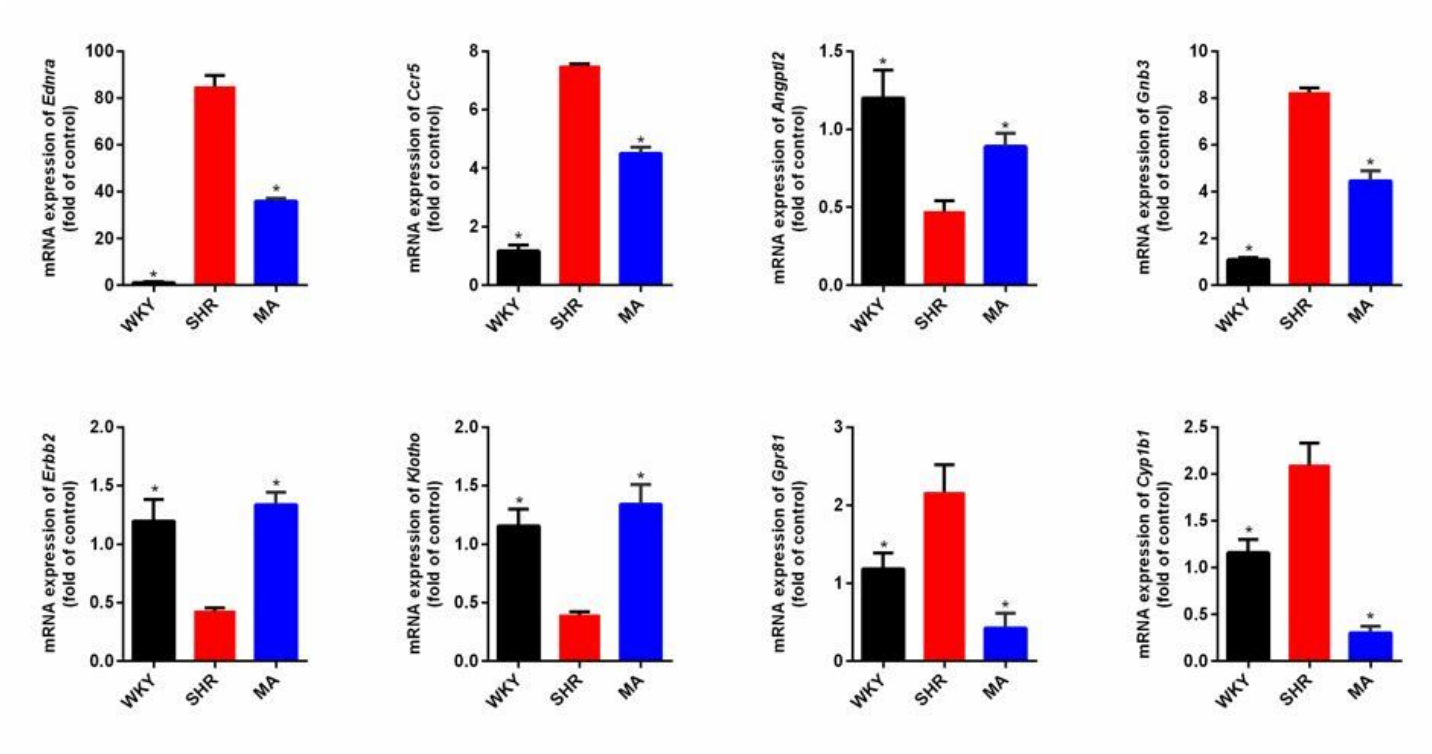

Figure 5

Validation of the up/downregulated genes using qRT-PCR. The loading control gene β-actin was used for normalization. Data are expressed as the mean ± SD. * $p < 0.05$ versus the SHR group.

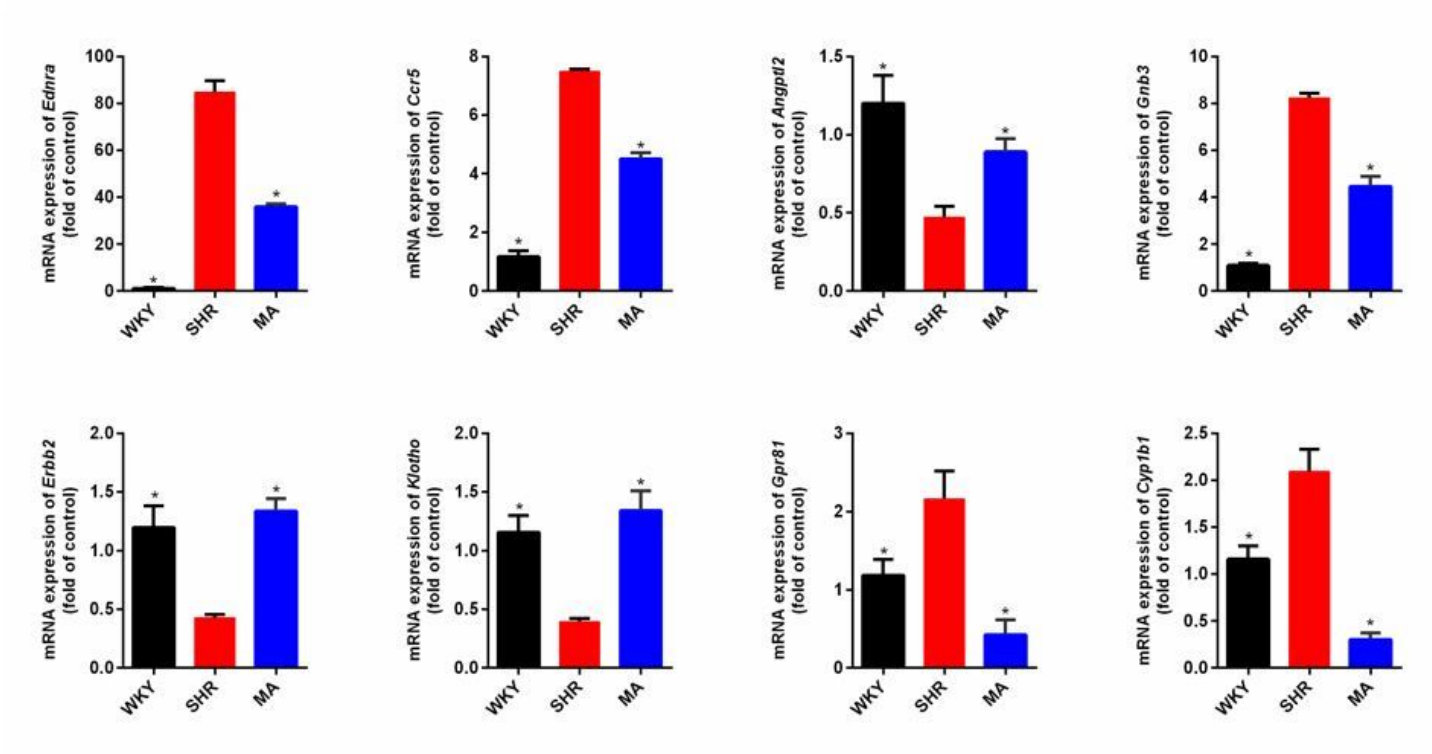

Figure 5

Validation of the up/downregulated genes using qRT-PCR. The loading control gene β-αctin was used for normalization. Data are expressed as the mean ± SD. * $p < 0.05$ versus the SHR group.

Supplementary Files

This is a list of supplementary files associated with this preprint. Click to download.

- Supplementarymaterials.pdf
- Supplementarymaterials.pdf